

## ANALYSIS OF THE PRESSURE DISTRIBUTION OF OIL FILM IN THE VARIABLE HEIGHT GAP BETWEEN THE VALVE PLATE AND CYLINDER BLOCK IN THE AXIAL PISTON PUMP

Tadeusz Złoto\*, Arkadiusz Nagórka \*\*

\*Institute of Machine Technology and Production Automation,  
Armii Krajowej Av. 21, 42-200 Częstochowa, Poland, e-mail:złoto@itm.pcz.czyst.pl

\*\*Institute of Computer and Information Sciences  
Częstochowa University of Technology

Dąbrowskiego Str. 73, 42-200 Częstochowa, Poland, e-mail: arkadiusz.nagorka@icis.pcz.czyst.pl

**Summary.** The pressure distribution of oil film at the smallest height of the gap occurring between the valve plate and cylinder block is presented as a variable depending on the geometrical and exploitation parameters of the axial piston pump. The analysis was performed using the finite element method implemented in a computer program developed by the authors of the present paper.

**Key words:** pressure distribution, variable height gap, axial piston pump, computer program

### INTRODUCTION

One of the kinematic pairs affecting the efficiency of an axial piston pump is the valve plate – cylinder block system. When the pump is operating a gap filled with oil of small height appears between the rotating cylinder block with the set of cylinders and the valve plate [Pasynkov 1976]. The gap can be either parallel [Stryczek 1995], which is the most desirable case, or of variable height [Pasynkov 1965], which results from the imbalance between the hydrostatic forces pressing the cylinder block and valve plate towards each other and forces pressing them apart from each other. The present paper deals with the latter case, i.e. the gap of variable height. We shall examine how the pressure distribution in the oil film in the gap where its height is the smallest varies according to the leveling of the cylinder block and exploitation parameters of the pump.

### APPROXIMATE SOLUTION OF THE REYNOLDS EQUATION USING THE FINITE ELEMENT METHOD

The operation of the valve plate-cylinder block system resembles the operation of a hydrostatic axial bearing [Ivantysyn and Ivantysynova 2001].

According to the hydrodynamic lubrication theory, distribution of pressure in the frontal gap of a hydrostatic bearing can be described by the Reynolds equation [Yampolskiy and Ablamskiy 1975, Pasyнков and Posvianskiy 1993]:

$$\frac{\partial}{\partial x} \left( \frac{h^3 \rho}{\mu} \frac{\partial p}{\partial x} \right) + \frac{\partial}{\partial y} \left( \frac{h^3 \rho}{\mu} \frac{\partial p}{\partial y} \right) = 6 \frac{\partial}{\partial x} (\rho u h) + 6 \frac{\partial}{\partial y} (\rho v h) + 12 \rho w \quad (1)$$

where:

- $p$  – the pressure in the bearing gap,
- $h$  – the gap height,  $\rho$  is the lubricating oil density,
- $\mu$  – the dynamic lubricant viscosity,
- $u, v, w$  – denote the components of peripheral velocity by the given angular velocity  $\omega$  and the radius vector  $r$  of the cylinder block with respect to the axes  $x, y, z$  in the Cartesian coordinate system.

The Reynolds equation (1) holds under the following assumptions:

- the flow in the frontal gap is laminar,
- fluid friction takes place between the cooperating surfaces,
- the lubricant is an incompressible Newtonian fluid,
- the pressure is constant in the direction orthogonal to the surface,
- the cooperating surfaces are rigid.

Analytical solution of equation (1) is quite complicated, particularly for surfaces of more complex shape. Therefore, the equation was solved numerically using the finite element method. In this method geometric domain  $\Omega$  under consideration is divided into finite elements, that is disjoint geometric figures of simple shape, such as triangles or quadrilaterals (Fig. 1).

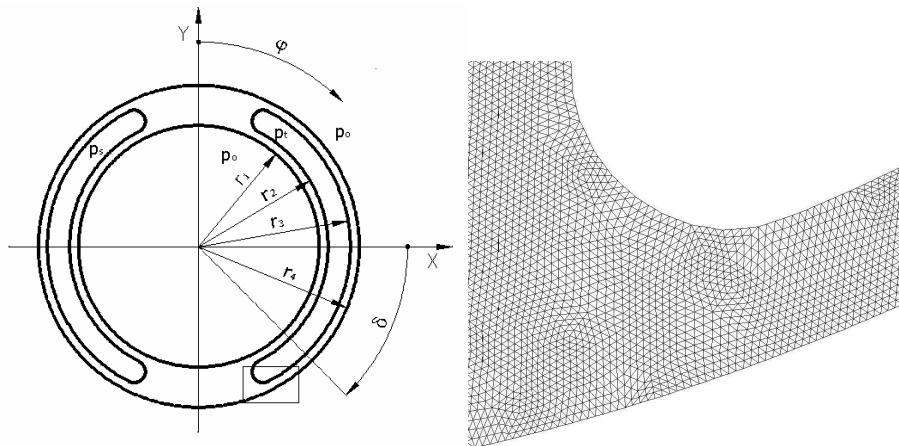


Fig. 1. Main dimensions of the computational domain of the valve plate and part of the finite element mesh

These simple figures constitute a mesh where their vertices are the mesh nodes. Approximate solution of equation (1) is represented as a linear combination of some functions  $N_j$  and values of the pressure  $p_j$  in mesh nodes

$$p(x, y) = \sum_{j=1}^L N_j(x, y) p_j \quad (2)$$

where:

$L$  – the number of nodes in the mesh,

$p_j$  – the unknowns of the problem and after they have been determined it is possible to calculate the pressure in any point of the domain,

$N_j$  –, called basis or shape functions, are used for interpolation of the pressure within a finite element.

The shape function  $N_j$ , associated with the node of the index  $j$ , has the property

$$N_j(x_k, y_k) = \begin{cases} 1, & j = k \\ 0, & j \neq k \end{cases} \quad (3)$$

i.e. it equals one in this node, whereas it is equal to zero in the other nodes. For the triangular element with linear interpolation, used in this work, plots of shape functions are presented in Fig. 2.

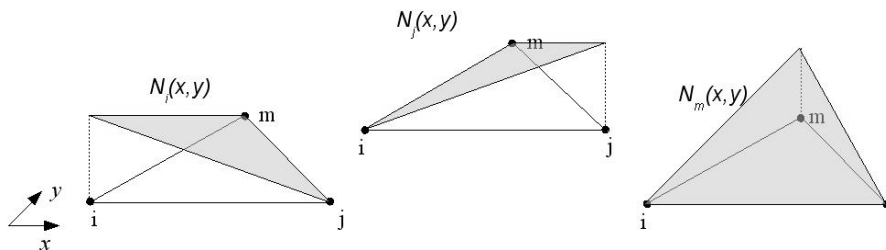


Fig. 2. Plots of nodal shape functions in a triangular finite element

Given that an element under consideration has vertices in nodes  $i, j, m$ , the shape function associated with the node  $i$  equals [Zienkiewicz and Taylor 2000]

$$N_i(x, y) = \frac{a_i + b_i x + c_i y}{2A} \quad (4)$$

where:

$$a_i = x_j y_m - x_m y_j, \quad b_i = y_j - y_m, \quad c_i = x_m - x_j,$$

$A$  – the element surface area.

The other shape functions can also be calculated from formula (4) after cyclic permutation of the indices, e.g. to  $j, m, i$ .

Approximate solution obtained numerically usually fails to satisfy the partial differential equation (1). The magnitude of this discrepancy can be measured by the residual, which is the result of the substitution of the approximate solution for the exact one. For the Reynolds equation the residual is given as

$$r = 6 \frac{\partial}{\partial x} (\rho u h) + 6 \frac{\partial}{\partial y} (\rho v h) + 12 \rho w - \frac{\partial}{\partial x} \left( \frac{h^3 \rho}{\mu} \frac{\partial p}{\partial x} \right) - \frac{\partial}{\partial y} \left( \frac{h^3 \rho}{\mu} \frac{\partial p}{\partial y} \right) \neq 0 \quad (5)$$

The Galerkin weighted residual [Zienkiewicz and Morgan 1983] method was applied in this work to derive finite element equations. It is required that

$$\int_{\Omega} r N_i dx dy = 0 \quad \text{for } i = 1, 2, \dots, L \quad (6)$$

i.e. that the residual be orthogonal to each shape functions defined in the mesh.

Substituting the residual (5) in the equation (6), integration by parts and some reordering results in the following system of equations

$$\int_{\Omega} \frac{h^3 \rho}{\mu} \left( \frac{\partial p}{\partial x} \frac{\partial N_i}{\partial x} + \frac{\partial p}{\partial y} \frac{\partial N_i}{\partial y} \right) dx dy = \int_{\Omega} N_i \left( 6 \frac{\partial}{\partial x} (\rho u h) + 6 \frac{\partial}{\partial y} (\rho v h) + 12 \rho w \right) dx dy, \quad i = 1, 2, \dots, L \quad (7)$$

Derivatives of the approximate solution with respect to spatial coordinates appear in equation (7). They can be represented using derivatives of the shape functions and the nodal pressure values as

$$\frac{\partial p}{\partial x} = \sum_{j=1}^N \frac{\partial N_j}{\partial x} p_j, \quad \frac{\partial p}{\partial y} = \sum_{j=1}^N \frac{\partial N_j}{\partial y} p_j \quad (8)$$

For triangular elements used in this paper derivatives of the shape functions are respectively equal to

$$\frac{\partial N_i}{\partial x} = \frac{b_i}{2A}, \quad \frac{\partial N_i}{\partial y} = \frac{c_i}{2A} \quad (9)$$

Substituting the derivatives from (8) into (9) gives the following system of algebraic equations

$$\sum_{j=1}^L p_j \int_{\Omega} \frac{h^3 \rho}{\mu} \left( \frac{\partial N_j}{\partial x} \frac{\partial N_i}{\partial x} + \frac{\partial N_j}{\partial y} \frac{\partial N_i}{\partial y} \right) dx dy = \int_{\Omega} N_i \left( 6 \frac{\partial}{\partial x} (\rho u h) + 6 \frac{\partial}{\partial y} (\rho v h) + 12 \rho w \right) dx dy, \quad i = 1, 2, \dots, L \quad (10)$$

This is a system of  $L$  equations with  $L$  unknowns  $p_j$ , which can be represented in a more compact manner in matrix-vector notation as

$$Ap = b \quad (11)$$

where:

$$a_{ij} = \int_{\Omega} \frac{h^3 \rho}{\mu} \left( \frac{\partial N_j}{\partial x} \frac{\partial N_i}{\partial x} + \frac{\partial N_j}{\partial y} \frac{\partial N_i}{\partial y} \right) dx dy, \quad i, j = 1, 2, \dots, L \quad (12)$$

$$b_i = \int_{\Omega} N_i \left( 6 \frac{\partial}{\partial x} (\rho u h) + 6 \frac{\partial}{\partial y} (\rho v h) + 12 \rho w \right) dx dy, \quad i = 1, 2, \dots, L \quad (13)$$

This system is global. Analogous local systems of equations can be written for all finite elements, with the only difference lying in summing in the range  $i = 1, 2, 3$  and in integration over the element area of only those shape functions that are associated with its nodes.

#### COMPUTER IMPLEMENTATION OF THE FINITE ELEMENT METHOD

The finite element method for the Reynolds equation was implemented in a computer program. It was written in the C++ programming language based upon an existing software library of reusable components facilitating programming of the finite element method [Nagorka and Sczygiol 2004].

Finite element computations usually consist of

- reading the mesh and problem data from files,
- building the system of equations (11) as the result of assembling contributions from individual elements,
- imposition of boundary conditions,
- solution of the resulting equation system,
- saving the results to files, visualization, etc.

Coefficients of the matrix and the right-hand side vector in equation system (11) involve integrals of shape functions or their derivatives, material data, gap height and velocity components. The derivatives in (12) can be calculated from formula (9) and are constant within an element. However, variation of the height  $h$  is non-polynomial and analytical evaluation of the integral (12) is troublesome. Similarly, derivatives of velocity and height in (13) make the integral difficult to evaluate. Therefore, numerical integration was used to calculate matrix and vector elements in system (11). Gaussian quadrature formulas were applied with points and weights taken from [Cools 2003].

The coefficient matrix in the system of equations (11) is sparse. Each matrix row corresponds to a single mesh node, and the number of non-zero coefficients in the row depends on the number of neighbor nodes connected with the given node by element edges, which is small. Keeping all the square matrix in memory would be waste of resources. In the computer program special data structures were applied to store only non-zero terms, thereby greatly reducing the memory consumption.

Solution of the system of algebraic equation (11) is by far the most time-consuming part of computations. Generally, the equations are nonlinear. However, in this work material properties were assumed to be independent of pressure, hence system (11) is linear. To solve such a system one of the iterative solution methods, namely the conjugate gradient method with the Jacobi preconditioner [Barrett *et al.* 1994] was applied. The advantages of this method are much more efficient when compared to classical direct methods, such as Gaussian elimination on dense or sparse matrices, and feasibility of efficient use of sparse matrix data structures.

The developed computer program accepts input data and saves the results in file formats compliant with a software package NuscaS [Sczygiol *et al.* 2002], used for mesh generation, preprocessing, visualization, etc.

The accuracy of the finite element solution depends on mesh density: the smaller the elements, the better accuracy. This is particularly important in place where rapid variation of pressure occurs, close to the site of the smallest bearing gap height. Simulations were performed on meshes from a sequence with increasing element density until convergence was reached, i.e. until the result on the two consecutive meshes were similar enough. Final computations were done on the densest mesh including 80194 nodes and 154336 triangular elements with linear interpolation of the pressure.

## SIMULATION RESULTS

Distribution of pressure in the oil film inside the variable-height gap on the valve plate was analyzed using the finite element method, the developed computer program and geometric and exploitation data of the valve plate-cylinder block system in an axial piston pump.

The following input parameters were assumed in the developed computational model (Fig. 1):

- in the pressure port the pressure  $p_t = 32$  MPa,
- in the suction port the pressure  $p_s = 0$  MPa,
- outside and inside the valve plate the pressure  $p_o = 0$  MPa,
- angular velocity of the cylinder block  $\omega = 157$  rad/s,
- dynamic viscosity of the oil  $\mu = 0.0252$  Pas,
- the angle of the smallest height of the gap with respect to the axis  $x$   $\delta = 0.785$  rad,
- the angle of the cylinder block with respect of the valve plate  $\varepsilon = 0.000523$  rad,
- minimal gap height  $h_{\min} = 3 \cdot 10^{-7}$  m
- characteristic radii of the valve plate are  $r_1 = 0.0284$  m,  $r_2 = 0.0304$  m,  $r_3 = 0.0356$  m, and  $r_4 = 0.0376$  m.

In Fig. 3 distribution of oil film pressure on the valve plate is presented. Pressure variation in the vicinity of the lowest bearing gap height is of greatest interest. In the confuser part of the gap (where the height decreases) an overpressure peak is visible, whereas in the diffuser part a negative pressure peak forms. Peripheral section at the radius 0.03715 m with the greatest pressure peaks is depicted in Fig. 4.

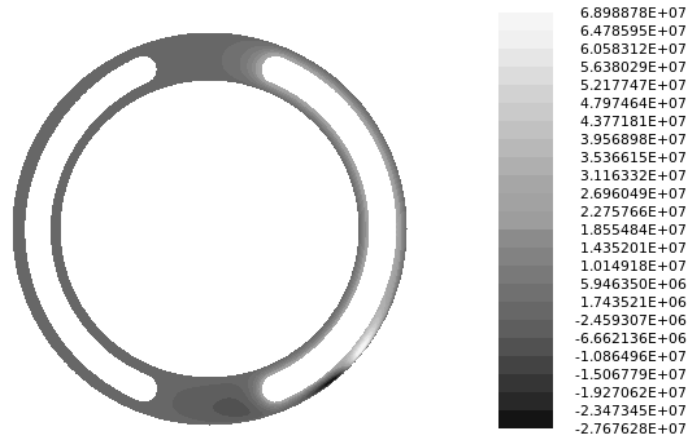


Fig. 3. Oil film pressure distribution on the valve plate

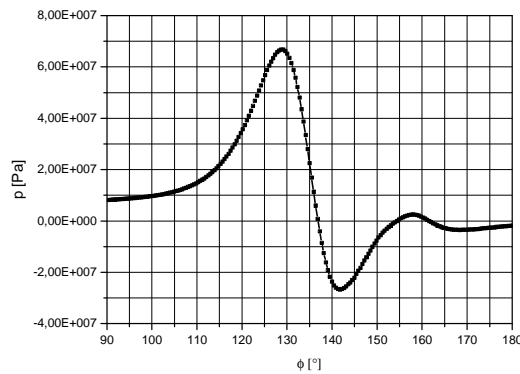


Fig. 4. Overpressure and negative pressure waveforms of the oil film in the vicinity of the smallest height gap of the circumferential section at the radius  $r = 0.03715$  m depending on the cylinder block revolution

In the analysis of the pressure distribution an influence of the geometrical and exploitation parameters of the cylinder block-valve plate system on the pressure increase and decrease in the smallest gap height area was taken into consideration

In Fig. 5 the effect of the cylinder block inclination with respect to the valve plate is shown. As the inclination angle increases, the peak values of the maximum pressure and negative pressure decrease. The greatest values occur for small angles  $\varepsilon$ .

In Figs. 6–7 the influence of exploitation parameters on the maximum and minimum pressure values is depicted.

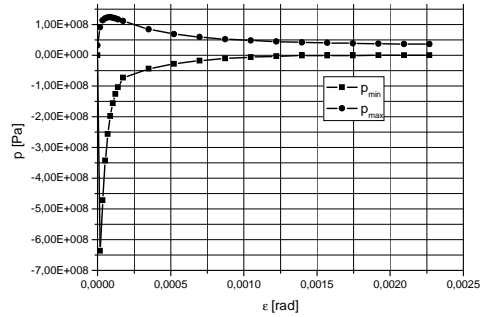


Fig. 5. Values of maximum and minimum pressure of oil film depending on the cylinder block inclination angle  $\varepsilon$

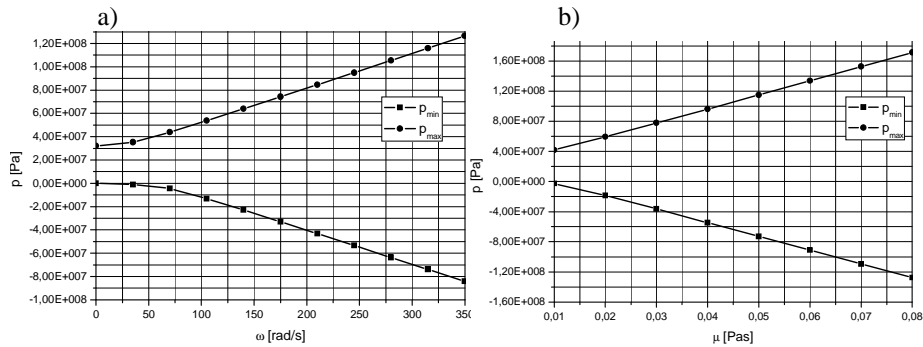


Fig. 6. Values of maximum and minimum pressure of oil film depending: a) on the cylinder block angular velocity  $\omega$ , b) on the dynamic viscosity coefficient  $\mu$  of oil

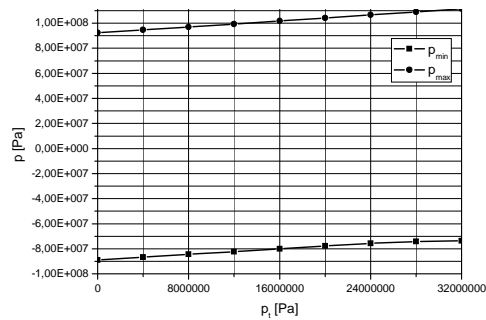


Fig. 7. Values of maximum and minimum pressure of oil film depending on the pump pressure  $p_t$

An increase in the angular velocity and in dynamic viscosity coefficient causes a linear increase in the values of the maximum and minimum pressure of the oil film. Changes in the pump pressure, however, only slightly affect the above mentioned pressures.

## CONCLUSIONS

The present investigations lead to the following conclusions:

1. The finite element method combined with numerical methods enables the solution of the Reynolds equation in order to determine the oil film pressure in variable height gaps between cooperating elements.
2. The distribution of the maximum and minimum pressures of the oil film in the area of the smallest height gap are dependent on the selected geometrical and exploitation parameters of the pump. As the inclination angle of the cylinder block decreases and the angular velocity and the dynamic oil viscosity coefficient increase, the values of the maximum and minimum pressures increase. Contrary to this, the pump pressure has little influence on the maximum and minimum pressures.

## REFERENCES

- Barrett R., Berry M., Chan T.F., Demmel J., Donato J., Dongarra J., Eijkhout V., Pozo R., Romine C., Vorst H.V. 1994: *Templates for the Solution of Linear Systems: Building Blocks for Iterative Methods*. 2nd Edition, SIAM, Philadelphia, PA.
- Cools R., 2003: An Encyclopaedia of Cubature Formulas J. Complexity, 19, 445–453.
- Ivantysyn J., Ivantysynova M., 2001: *Hydrostatic Pumps and Motors*. Akademia Books International. New Delhi.
- Nagorka A., Sczygiol N., 2004: Implementation aspects of a recovery-based error estimator in finite element analysis, [in:] *Lecture Notes in Computer Science*, 3019, Wyrzykowski R. *et al.* (Eds), 722–729.
- Pasynkov R. M. 1976: Vliyanie pierekosa cylindrovokho bloka na rabotu torcovokho raspriedielitiela akcyalno-porshnievoy hidromashiny. *Viesnik Mashinostroyeniya* 10, 49–50.
- Pasynkov R. M. 1965: K raschietu torcovykh raspriedieliteley akcyalno-porshnievykh nasosov. *Viesnik Mashinostroyeniya* 1, 22–26.
- Pasynkov R. M., Posvianskiy V. S. 1993: Chisliennoye rieshenie uravnieniya Reynoldsa s uchetom pieremiennoy vyaskosti djidkosti (v prilodjeni k torcovym raspriedieliteliam, uplotnieniam i upornym podshipnikam skoldjeniya). *Viesnik Mashinostroyeniya* 9, 26–29.
- Sczygiol N., Nagórka A., Szwarz G., 2002: NuscaS – autorski program komputerowy do modelowania zjawisk termomechanicznych krzepnięcia. *Polska metalurgia w latach 1998–2002*. Wydawnictwo Naukowe AKAPIT, 243–249.
- Stryczek S., 1995: *Napęd hydrostatyczny*, tom 1. WNT, Warszawa.
- Yampolskiy S. L., Ablamskiy V. A. 1975: O kriteriyakh podobija hidrodinamicheskikh podshipnikov. *Mashinoviedeniye* 2, 72–78.
- Zienkiewicz O.C. and Morgan K., 1983: *Finite Elements and Approximation*. John Wiley & Sons, Inc.
- Zienkiewicz O. C., Taylor R.L., 2000: *The Finite Element Method*. Butterworth-Heinemann. Oxford.